Observation of Vortex Coalescence, Vortex Chains and Crossing Vortices in the Anisotropic Spin-Triplet Superconductor Sr_2RuO_4

K. Hasselbach [a,*], V.O. Dolocan [a,1], P. Lejay [a] Dominique Mailly [b]

[a] *CRTBT-CNRS, BP 166X, 38042 Grenoble, France*
[b] *LPN-CNRS, Route de Nozay, 91460 Marcoussis, France*

Abstract

Scanning μSQUID force microscopy is used to study magnetic flux structures in single crystals of the layered spin triplet superconductor Sr_2RuO_4. Images of the magnetic flux configuration above the $\vec{a}\vec{b}$-face of the cleaved crystal are acquired, mostly after field-cooling the sample. For low applied magnetic fields, individual vortices are observed, each carrying a single quantum of flux. Above 1 gauss, coalescence of vortices is discovered. The coalescing vortices may indicate the presence of domains of a chiral order parameter.

When the applied field is tilted from the $\vec{c}$-axis, we observe a gradual transition from vortex domains to vortex chains. The in-plane component of the applied magnetic field transforms the vortex domains to vortex chains by aligning them along the field direction.This behavior and the inter-chain distance varies in qualitative agreement with the Ginzburg Landau theory of anisotropic 3D superconductors. The effective mass anisotropy of Sr_2RuO_4, γ=20, is the highest observed in three dimensional superconductors.

When the applied field is closely in plane, the vortex form flux channels confined between the crystal-layers. Residual Abrikosov vortices are pinned preferentially on these channels. Thus the in-plane vortices are decorated by crossing Abrikosov vortices: two vortex orientations are apparent simultaneously, one along the layers and the other perpendicular to the layers.

Key words: superconductivity, Sr_2RuO_4, magnetic microscopy,
PACS: 74.20.Rp, 74.25.Qt, 74.70.Pq, 85.25.Dq

1. Introduction

Sr_2RuO_4 is a tetragonal, layered perovskite superconductor with a superconducting transition temperature (T_c) of 1.5 K [1]. Sr_2RuO_4 has been a subject of intensive interest in recent years because of the theoretical suggestion [2,3] that Sr_2RuO_4 is an odd-parity, spin-triplet superconductor. Abundant experimental evidence supporting the theoretical prediction has been obtained, as summarized recently [4,5]. A very recent phase-sensitive experiment [6] has established the odd-parity pairing symmetry in Sr_2RuO_4 by measuring the quantum interference pattern in Superconducting Quantum Interference Devices (SQUIDs) consisting of Sr_2RuO_4 and $Au_{0.5}In_{0.5}$, an s-wave superconductor. In addition, muon spin rotation (μSR) experiments have revealed [7] the presence of spontaneous currents in the superconducting Sr_2RuO_4, indicating the breaking of time reversal symmetry (TRS) below T_c. The TRS breaking implies that the Cooper pair has an internal orbital moment (chirality) giving rise to a superconducting order parameter with multiple components.

The crystal structure and the thermodynamic properties of the superconductor restrain the choice of the order parameter. The orbital component of the order parameter of the form, ($p_x \pm ip_y$) is compatible with most experiments. The two possible realisations of the superconducting order parameter, $p_x + ip_y$ (p+) and $p_x - ip_y$ (p-), represent two possible chiral states [8] which are energetically degenerate. Consequently the presence of domains is expected in which the Cooper pairs posses different orbital angular momenta. Building on this form of the order parameter, the magnetization processes were explored by numerical simulations [9,10]. In a magnetic field the degeneracy between p+ and p- domains is lifted, favoring a domain with the Copper pair orbital moment aligned with the field. The favored domains will have a higher critical field H_{c2}, and a lower H_{c1}. Consequently, vortices will first appear in these domains.

* Corresponding author.
Email addresses: klaus.hasselbach@grenoble.cnrs.fr (K. Hasselbach), dolocan@cpfs.mpg.de (V.O. Dolocan).
[1] Present address: Max Plank Institute for Chemical Physics of Solids, 40 NöthnitzerStr., 01187 Dresden, Germany

At the interface between the domains of opposite chiralities, walls will form [11]. The presence of domain walls has considerable influence on the vortex motion and pinning. For example, flux penetration should take place preferentially along the domain walls. These walls will act as preferential pinning sites for vortices. Vortices at these sites could decompose into fractional vortices decorating the domain walls. In analogy with the case of superfluid ^{3}He-A decorated domain walls are called vortex sheets [12,13].

The magnetic properties of superconductors depend strongly on their crystalline and electronic anisotropy. The general theoretical approach on vortex matter is based on the anisotropic Ginzburg-Landau (GL) theory. There the anisotropy is expressed in terms of the effective mass of the electron. For layered anisotropic superconductors, the out of plane effective mass m_c is much larger than the in plane effective masses ($m_c >> m_{ab}$). To describe this anisotropy the parameter $\gamma=(m_c/m_{ab})^{1/2}=\lambda_c/\lambda_{ab}$[14] is used. For example in $NbSe_2$ γ=3.3, in YBCOγ=5-8 and in BSCCO γ is higher than 150, γ being dependent on the oygen doping of the high T_c superconductors. Sr_2RuO_4 has a also a layered structure, the RuO_2 planes are separated by 12.74 Å and has highly anisotropic properties[4]. Sr_2RuO_4 has a γ value of 20 situating it between YBCO and BSCCO on the anisotropy scale. We expect Sr_2RuO_4 to act more like a 3D superconductor as the c-axis parameter is 3 times smaller than the coherence length ξ_c. The Ginzburg-Landau parameter $\kappa = \lambda/\xi$ is around 2.3 when the magnetic field is applied along the c-axis direction and 46 for the in-plane direction. The physical properties of Sr_2RuO_4 are very rich due to its unconventional mecanism of superconductivity and its anisotropy. Scanning magnetic probe microscopy[15,16]. is a means of choice to study this interplay.

2. μ SQUID Force microscopy and crystals

We use for magnetic imaging a high resolution scanning μSQUID microscope (SμSM)[17] working in a dilution refrigerator. The SμSM has an aluminum μSQUID as pickup loop of 1.2μm diameter. The critical current of the μSQUID is a periodic function of the magnetic flux emerging perpendicularly from the sample surface. The images shown are maps of the critical current value of the μSQUID while it scans the surface. The magnetic fields are applied by a solenoid and a rotatable Helmholtz coil, the copper coils are at room temperature. The solenoid axis is parallel to the ab face of the sample and the Helmholtz coil generates a field perpendicular to the solenoid axis. Adjusting the relative angle and the magnitude of the two fields allows us to point the resultant field along any direction. The Sr_2RuO_4 single crystal was grown by a floating zone technique using an image furnace [18,19]. Specific heat measurements of crystals taken from the same single-crystal rod showed volume superconductivity below a temperature of 1.31 K and a transition width of less than 0.1K. We used 2 different samples of plate like shape of this crystal, one having a thickness of 0.5mm with an estimated demagnetization factor, N of 0.9 (sample 1) and the other 0.6mm with N =0.7 (sample 2). The sample is cleaved along the ab -plane and AFM images show flatness down to the order of 6 $\AA$ (Fig. 1), about twice as flat as surfaces of $NbSe_2$).

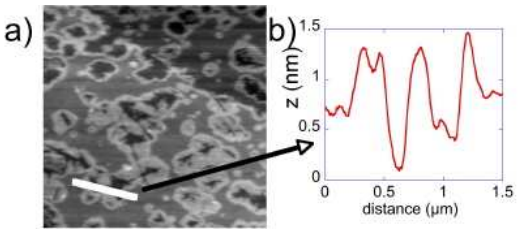

Fig. 1. (a)AFM Image of the surface of cleaved Sr_2RuO_4(b)Line scan as indicated, the roughness is of the order of half the unitcell.

3. Coalescence, flux domains and crossing vortices

During the imaging, the μSQUID moved in a plane above a cleaved ab surface of the single crystal of Sr_2RuO_4. Individual vortices are seen [16] after cooling the crystal (sample 1) in a magnetic field of 0.1G applied along the c-axis. The vortices disappear completely above T = T_c = (1.35±0.05)K, in agreement with the T_c value determined previously in specific heat measurements. At these low fields Sr_2RuO_4 behaves as a usual type-II superconductor. The images of Fig. 2 were obtained after field cooling (FC) sample 2 in fields between 2 and 7 gauss to a temperature of 0.35K. At 2 gauss applied field, Fig. 2(a), vortices are distinct, some of them are close together, at 6 gauss Fig. 2(b) a higher density of individual vortices is detected, locally coalescing flux regions form, and as the field increases further to 7 gauss, Fig. 2(c) the individual vortices have melted into flux domains. For comparison, we imaged a conventional s-wave superconductor $NbSe_2$ having a T_c of 7.2K. $NbSe_2$ is a layered material, it is weakly anisotropic with an effective mass anisotropy (λ_c/λ_{ab}) of 3.3. The penetration depth for applied fields along c-axis λ_{ab} is 0.15μm comparable with λ_{ab} of Sr_2RuO_4. A hexagonal vortex lattice is readily observed by the μSFM Fig. 2(d), after field cooling the sample in 5 gauss. The vortices are clearly distinct from one another. When the field is further increased the vortices in $NbSe_2$ approach so close that μSFM can't resolve the vortices anymore and the flux appears homogenous. The case of Sr_2RuO_4 is different: Instead of the formation of a vortex lattice we observe vortex coalescence. The threshold value of the applied field at which the vortices coalesce depends on the thickness of the sample. A complete collapse of the vortices into one single domain is not observed, probably due to the presence of weak barriers in the material.

Domain walls delimiting regions with angular momentum $l_z = \pm 1$ ($\widehat{l}$ is parallel to the c-axis) could provide the scenario for weak intrinsic pinning at low magnetic fields.

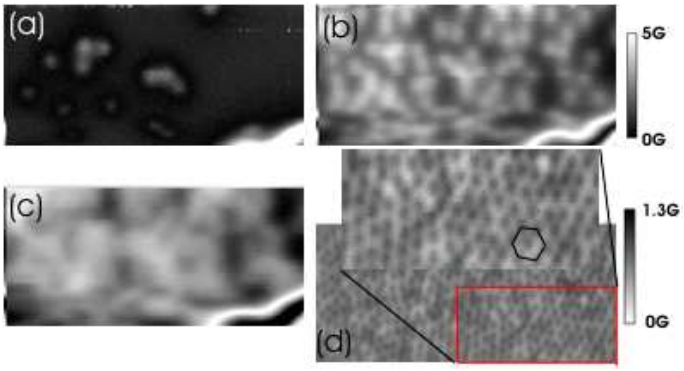

Fig. 2. Comparison between $NbSe_2$ and Sr_2RuO_4 for magnetic fields applied perpendicular to the ab plane. (a) A μSFM image after field cooling Sr_2RuO_4 in a field of 2 gauss, (b) in 6 gauss and (c) in 7 gauss. The imaging temperature is 0.35K for all images. Coalescence of vortices is observed. (d) A μSFM image of a vortex lattice in $NbSe_2$. The data is acquired after field cooling the $NbSe_2$ crystal in 5 gauss at a temperature of 1.1K. The inset shows the hexagonal order of the lattice. For all images the imaging area is 62μm $\times 30\mu$m.

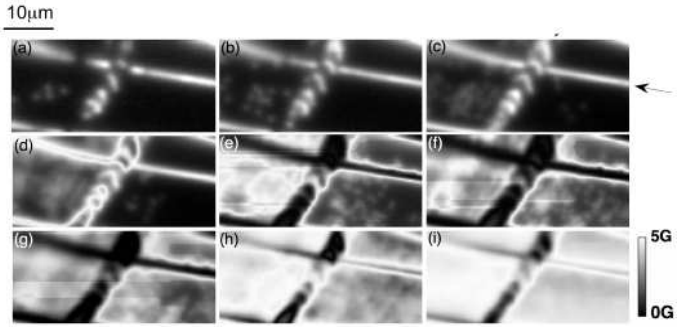

Fig. 3. μSFM image of 62μm $\times 30\mu$m after field cooling Sr_2RuO_4 in (a)2G, (b)3G, (c)4G, (d)8G, (e)9G, (f)10G, (g)11G, (h)20G, (i)50G at 0.4 K H//c. Line defects, groves, (arrow) delimit regions of the crystal. The vortex distribution is very different between regions separated by the defects.

The difference of free energy under magnetic field between the two states [9,10] may make that vortices appear preferentially in domains of one type. This is in qualitative agreement with our observations, as we observe flux filled and flux free regions. By accident we imaged an area delimited by line defects (grooves) Fig. 3. We acquired images after field-cooling in fields between 2 and 50 gauss. In the normal state the magnetic flux is equally distributed throughout the sample, upon field-cooling into the superconducting state the flux in the center of the sample has to move out (Meisssner eeffect), or it stays pinned and transforms to quantized vortices. Here we observe that the region on the upper left side retains flux much more readily than the region on the other side of the line defect. Only after cooling in fields as high as 8 gauss vortices remain in the region on the right side. Different is also the high contrast along the edge of this region Fig. 3 e-g). These observations agree with a scenario of pinning of domain walls on linear defects and thus delimiting regions with cooper pairs of different angular. This experiment indicates tentatively a way to study the order parameter domains, though a complete picture of the interaction between vortices, domain walls seperating regions of different chirality, shielding currents and surface defects has yet to be established both experimentally and theoretically. There should be a difference between field cooled (FC) and zero-field cooled (ZFC) experiments. Under ZFC conditions, domains of each chirality should be equally present. Upon subsequent field increase the vortex should penetrate by the domain walls and then enter from the edge preferentially in the p- wave domain. We made ZFC experiments and increased the applied field subsequently. At fields less than H_{c1} we observe only a few single vortices, the shielding currents at the surface retain the vortices, while above H_{c1}, at about 30 Gauss, vortices penetrate massively into the center of the sample.

How strongly are these domains attached to the crystal? In order to examine the stability of the domain configuration the in-plane field was raised while the c-axis field was kept constant. Fig. 4 shows for increasing in-plane fields how the condensed vortex structures rearrange freely in order to accommodate the experimental conditions: For zero gauss in plane field and 2 gauss FC applied parallel with c-axis in the sample 1 we see only domains of flux, Fig. 4(a). The difference in flux density between the bright (vortex) and the dark (vortex-free) regions is 3.5 gauss. Integration of the flux pattern gives an average field of 1.4±0.2 gauss at the μSQUID, close to the applied field of 2 gauss, the vortices are condensed in domains, leaving entire superconducting regions empty of flux.

At 5 gauss in-plane applied field the flux domains become slimmer and above 10 gauss the flux domains are seen to evolve into line-shaped structures. The number of flux domains was found to increase in a regular fashion with the in-plane field amplitude. This regular increase of the flux domain density and their temperature evolution (data not shown) suggest that the flux structures are unrelated to any structural defects in the crystal as defect pinning [20] of vortices would interfere with regularly spaced vortex pattern.

The line-shape flux structures evoke vortex chains observed in decoration experiments of $YBa_2Cu_3O_{7+\delta}$ [21] and $Bi_2Sr_2CaCu_2O_{8+\delta}$ [22]. There vortex chains appear when the applied field is close to the in-plane direction of the anisotropic superconductor. Sr_2RuO_4 has an effective mass anisotropy 6 times higher than $NbSe_2$ and 4 times higher $YBa_2Cu_3O_{7+\delta}$ but lower than $Bi_2Sr_2CaCu_2O_{8+\delta}$. Therefore the arrangement of the domains in lines may be driven by anisotropy. The attraction between vortices in anisotropic superconductors comes from the misalignment between the vortex axis (B) and the direction of the applied field (H) giving raise to a net transverse magnetization M. This attractive interaction [23] between the vortices is directed along the plane spanned by the anisotropy axis and the in-plane applied field. We observe also that the linear pattern follow the direction of the applied field when the field is rotated in the ab plane (images not shown), this

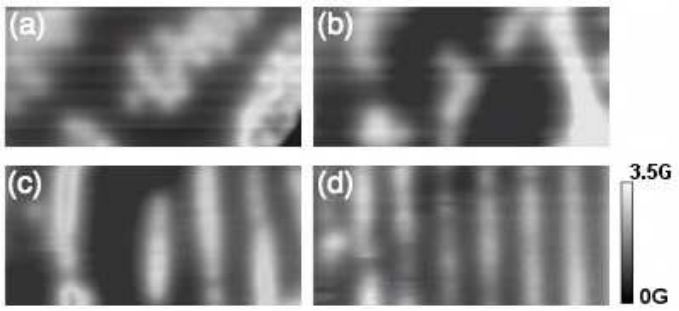

Fig. 4. SμSM images of flux domains in Sr_2RuO_4 at T = 0.36K after field cooling at various fields. In all cases, the magnetic field amplitude applied along c-axis ($H_\perp$) was kept constant at 2G while in-plane field (H_{ab}) was (a) 0G, (b) 5G, (c) 10G, (d) 50G. The imaging area is 31μm × 17μm. Field scale in gauss is shown on the right; dark regions are superconducting vortex free regions.

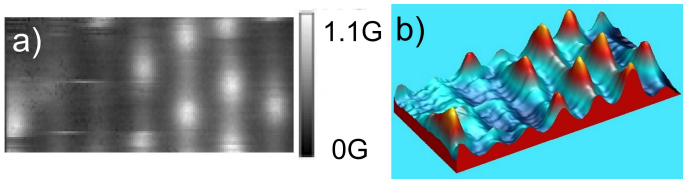

Fig. 5. Crossing vortices in Sr_2RuO_4. Figure (a) 10 G FC and increased to 50 G at low T. The magnetic scale is shown on the right. The dimensions are 31μm×15μm and the imaging temperature is 0.35K. The tilting angle is 87°. The (b) image is the 3D representation of the image (a).

proofs that the coalescence of the vortices in domains does not originate from defects as the magnetic energies in play can align these domains as vortex chains.

In isotropic superconductors at low tilted fields the flux lines penetrate parallel to each other and with the average field in the sample and arrange in a pattern that minimizes the interaction energy. If the superconductor is strongly anisotropic the free energy of the vortex state has two local minima and consequently a flux line can penetrate in two distinct directions in the material. For high anisotropy only flux lines that are nearly parallel or perpendicular to the layers are stable [24]. This model predicted that two types of vortices may be observed in Sr_2RuO_4, formed by two interpenetrating lattices, a lattice of vortices parallel to the layers and crossing vortices that are nearly parallel to the c-axis. We undertook measurements changing the applied magnetic field while the sample is in the superconducting state Fig. 5. The magnetic field component parallel to the plane is higher than the first critical field H_{c1} in the in-plane direction (H_{c1}^{ab}=10G), while the perpendicular component is lower than H_{c1}(H_{c1}^{c}=50G). We observe crossing vortices decorating flux channels Fig. 5.

4. Conclusion

We observe vortex coalescence and spatially dependent flux pinning, consistent with what might be expected from a chiral order parameter in Sr_2RuO_4. Tilting the magnetic field, anisotropy effects become important so the vortices try to align along the field direction, forming vortex chains. We observe the simultaneous presence of two vortex orientations in the crystal, one long the planes, flux channels, and one perpendicular to it, attributed to the decoration of in-plane flux channels by Abrikosov vortices.

5. Acknowledgments

We thank O. Fruchard for his help in acquiring the AFM images of the crystal surfaces.

References

[1] Y. Maeno, H. Hashimoto, K. Ioshida, S. Nishizaki, T. Fujita, J. Bednorz, F. Lichtenberg, Nature 372 (1994) 532–534.
[2] T. M. Rice, M. Sigrist, J. Phys.:Condens. Mat. 7 (1995) L643–L648.
[3] G. Baskaran, Physica Ba B 223 (1996) 490.
[4] A. P. Mackenzie, Y. Maeno, Rev. Mod. Phys. 75 (2003) 657–712.
[5] Y. Maeno, T. M. Rice, M. Sigrist, Phys. Today 54 (2001) 42.
[6] K. D. Nelson, Z. Q. Mao, Y. Maeno, Y. Liu, Science 306 (2004) 1151–1154.
[7] G. M. Luke, Y. Fudamoto, K. M. Kojima, M. I. Larkin, J. Merrin, B. Nachumi, Y. J. Uemura, Y. Maeno, Z. Q. Mao, Y. Mori, H. Nakamura, M. Sigrist, Nature 394 (1998) 558–561.
[8] V. P. Mineev, K. V. Samokhin, Introduction to unconventional Superconductivity, Gordon and Breaches Science Publishers, 1998.
[9] M. Ichioka, K. Machida, Phys. Rev. B 65 (2002) 224517.
[10] M. Ichioka, Y. Matsunaga, K. Machida, Phys. Rev. B 71 (2005) 172510.
[11] M. Sigrist, D. F. Agterberg, Prog. Theor. Phys. 102 (1999) 965–981.
[12] Y. Matsunaga, M. Ichioka, K. Machida, Phys. Rev. Lett. 92 (2004) 157001.
[13] U. Parts, E. V. Thuneberg, G. E. Volovik, J. H. Koivuniemi, V. M. H. Ruutu, M. Heinilä, J. M. Karimäki, M. Krusius, Phys. Rev. Lett. 72 (24) (1994) 3839–3842.
[14] J. R. Clem, Supercond. Sci. Tech. 11 (1998) 909–914.
[15] A. Grigorenko, S. Bending, T. Tamegai, S. Ooi, M. Henini, Nature 414 (2001) 728–731.
[16] V. O. Dolocan, C. Veauvy, F. Servant, P. Lejay, K. Hasselbach, Y. Liu, D. Mailly, Physical Review Letters 95 (9) (2005) 097004.
[17] C. Veauvy, K. Hasselbach, D. Mailly, Rev. Sci. Inst. 73 (2002) 3825–3830.
[18] F. Servant, J. Brison, A. Sulpice, C. Opagiste, V. Madigou, P. Lejay, Journal of Crystal-Growth 275 (2005) e739–43.
[19] F. Servant, Ph.D. thesis, Universite Joseph Fourier, Grenoble, France (2002).
[20] D. A. Huse, Phys. Rev. B 46 (1992) 8621–8623.
[21] P. L. Gammel, D. J. Bishop, J. P. Rice, D. M. Ginsberg 68 (1992) 3343–3346.
[22] C. A. Bolle, P. L. Gammel, D. G. Grier, C. A. Murray, D. J. Bishop, D. B. Mitzi, A. Kapitulnik 66 (1) (1991) 112–115.
[23] A. I. Buzdin, A. Y. Simonov, JETP Letters 51 (1990) 191–195.
[24] A. Sudbo, E. H. Brandt, D. A. Huse, Phys. Rev. Lett. 71 (1993) 1451–1454.